energies

MDPI

Article

A Comprehensive Study on DES Pretreatment Application to Microalgae for Enhanced Lipid Recovery Suitable for Biodiesel Production: Combined Experimental and Theoretical Investigations

Michele Corneille Matchim Kamdem [1,*], Aymard Didier Tamafo Fouegue [2] and Nanjun Lai [3,†]

[1] College of Chemistry and Chemical Engineering, Southwest Petroleum University, Chengdu 610500, China
[2] Department of Chemistry, Higher Teacher Training College, University of Bertoua, Bertoua P.O. Box 652, Cameroon
[3] Oil and Gas Field Applied Chemistry Key Laboratory of Sichuan Province, Southwest Petroleum University, Chengdu 610500, China
* Correspondence: michelematchim@gmail.com
† Deceased author.

Abstract: Cell wall disturbance is an important step in the downstream process of improving the efficiency of lipid extraction from microalgae. Surfactants have been proven to be efficient alternatives to organic solvents in the extraction process. In this study, an effective approach involving deep eutectic solvent (DES) (choline chloride and carboxylic acids) treatment supplemented with surfactants has been developed to disrupt the cell walls of microalgae and increase the extraction of lipids suitable for biodiesel production. A combination of polar and non-polar solvents (ethyl acetate and n-butanol) was used for the lipid extraction process. Microalgae biomass pretreated with choline chloride malonic acid supplemented with the surfactant hexadecyl trimethylammonium chloride (HTAC) showed the best results, improving lipid extraction by 12.365%. Further elucidation of the detailed mechanism behind the cell disruption of the microalga wall by DES was achieved using density functional theory (DFT) methods. The DFT calculations revealed that hydrogen bonds between the chloride ion of the DES and hydrogen bond donor (HBD) molecules are key factors dominating the destruction of the cell wall structure of *Chlorella pyrenoidosa*. The optimization of lipid extraction was performed through a single-factor experiment, which included the effects of different variables (time, temperature, dosage of surfactant, and ratio of n-butanol to ethyl acetate). An extraction period of 60 min at 80 °C with a surfactant concentration of 0.5% at a 1:2 ratio of n-butanol to ethyl acetate was found to produce the maximum lipid yield (16.97%). Transesterification reactions were used to obtain fatty acid methyl esters from the optimized extracted lipids. Thus, it was determined that C16:0 (20.04%), C18:2 (29.95%), and C18:3 (21.21%) were the most prevalent fatty acids. The potential for producing biodiesel from *C. pyrenoidosa* was validated by the high yields of C18 fatty acid methyl esters, and the properties of biodiesel are within the European and US standards.

Keywords: microalgae; cell wall; lipid extraction; deep eutectic solvent; pretreatment; density functional theory

Citation: Matchim Kamdem, M.C.; Tamafo Fouegue, A.D.; Lai, N. A Comprehensive Study on DES Pretreatment Application to Microalgae for Enhanced Lipid Recovery Suitable for Biodiesel Production: Combined Experimental and Theoretical Investigations. *Energies* **2023**, *16*, 3806. https://doi.org/10.3390/ en16093806

Academic Editors: Antonio Zuorro, Hongfang Lu, Enbin Liu, Shanbi Peng and Chengyong Li

Received: 28 March 2023
Revised: 24 April 2023
Accepted: 26 April 2023
Published: 28 April 2023
Corrected: 17 May 2024

1. Introduction

Due to the current energy crisis, global environmental problems, and the finite supply of fossil fuels, the renewable energy sector has become a trending topic. Biofuels are renewable energy sources that can be produced using a wide variety of plant and animal byproducts and waste products. The use of land for biomass production at the expense of maintaining ecosystem services or providing food has been a source of concern for scientists, environmentalists, and government regulators. Due to these concerns, more

attention is being paid to eukaryotic photosynthetic microalgae as a source of biomass for the production of biofuels [1].

Compared to conventional crops, microalgae offer several advantages in terms of high photosynthetic efficiency, carbon sequestration rates, lipid yields, and environmental adaptation with little or no impact on arable land or food supplies, which are all necessary for the manufacture of biofuels and other value-added industrial chemicals [2]. The lipids in microalgae are the main targets in the manufacture of biofuel, the latter of which is intended to be a sustainable and ecological alternative to fossil fuel. Some species are attractive potential biodiesel feedstocks because of their high lipid content (between 20 and 70%). Biodiesel numbers among the biofuels that have received the most attention among the numerous biofuels that can be produced from algae [3]. However, the biodiesel market faces a large obstacle due to the difficulty and expensiveness of extracting lipid from microalgae cells. Extractions of lipid from microalgae biomass have been performed using several methods [1]. To enhance lipid production, the thick cell walls of microalgae, which are composed of complex polysaccharides, must be weakened during the pretreatment step.

Cell disruption methods are classified into several types. Biochemical methods (such as alkali/heat or enzymatic) and physical treatments (such as bead beating, osmotic shock, autoclaving, sonication, and microwaving) have been tested for the purpose of improving lipid extraction from a variety of species. These conventional cell disintegration methods have drawbacks, such as high energy demands and scalability problems due to harsh conditions [4]. Additionally, the lipid extraction method from wet or dry algae entails the extensive use of organic solvents [5]. Alternative methods for reducing the number of organic solvents used in algal lipid extraction should be developed, especially given the high toxicity of some polar solvents. Surfactants with a hydrophobic tail and a hydrophilic head have been shown to interact with algal cell membranes and aid in cell wall disintegration [6]. In addition to their role in cell disruption, surfactants can be replaced by organic solvents for lipid extraction [7].

A novel class of environmentally friendly solvents called deep eutectic solvents (DESs) could solve the problems related to high cost, environmental risks, and the other drawbacks of conventional solvents, while simultaneously decelerating the degradation of target lipids that takes place at the high temperatures required for organic solvents. Recently, a number of studies have reported biomass processing with respect to the extraction of biomass components, i.e., phenolic compounds, using DES [8,9]. Ngatcha et al. [10] employed an ultrasonication-assisted DES treatment and increased the method's lipid extraction efficiency from 2.27% to 9.6%. Lu et al. [11] reported a DES pretreatment for microalgae biomass, wherein the amount of lipids significantly increased from 52.03% to 80.9%. Hence, judging by the results of these studies, DESs could be used for the dissolution and separation of microalgae biomass for the extraction of useful biomolecules. However, the mechanism behind DES-mediated pretreatment for extraction is unknown.

Therefore, it is highly important to optimize microalgae biomass pretreatment and determine the molecular mechanism responsible for the process to obtain maximum yields during extraction. The computationally based Density Functional Theory (DFT) simulation approach has proven indispensable in this area. For example, DFT computations and MD simulations were used by Mohan et al. [12] to study the dissolution of glucose in DESs based on tetrabutylammonium bromide. These methodologies enabled the investigation of the interactions between glucose and the DES. Thus, the hydrogen bond donor (HBD) molecules and the anion of the hydrogen bond acceptor with glucose govern the dissolution of glucose from lignocellulosic biomass. However, in the case of microalgae macromolecule extraction followed by DES pretreatment, DFT simulations are rarely employed to understand the molecular process and phase behavior of the system during pretreatment and extraction. Only a few studies are available regarding biomass treatments that use DESs to improve the yield of extraction [13]. In addition, this study attempts to elucidate the mechanisms of deep-eutectic-solvent-mediated microalgae cell wall disruption to enhance lipid extraction when using DFT simulations and experimental approaches.

In the present paper, choline-chloride and carboxylic-based (formic acid (FA), acetic acid (AA), and malonic acid (MA)) DESs were employed for the pretreatment of microalgae biomass to promote cell disruption for lipid extraction. To the best of our knowledge, the DESs ChCl:FA and ChCl:MA have never been used at the pretreatment stage to improve the yield of lipid extraction from *Chlorella pyrenoidosa*. The choice of *Chlorella pyrenoidosa* was made based on its good FAME profiles, which were previously reported by Liang and coworkers [14]. A combination of polar and non-polar solvents (ethyl acetate and n-butanol) and surfactants acting as a co-solvent were used in the lipid extraction step. Moreover, DFT simulations were performed to obtain more detailed information at the nano-scale on the mechanism behind the disintegration of the microalgae biomass during pretreatment and to understand the cellulose–DES interactions. Different parameters (temperature, time, the n-butanol/ethyl acetate ratio, and the dosage of surfactant) influencing the extraction process were explored through a single-factor experiment to determine the optimal conditions for lipid extraction. Moreover, the extracted lipid was subjected to transesterification, and the quality of the biodiesel produced was determined in comparison with European and US standards.

2. Materials and Methods

2.1. Material

Tianjin Norland Biotech Co., Ltd., located in Tianjin, China, supplied the *Chlorella pyrenoidosa* biomass. After 24 h in a vacuum oven set to 60 °C, the biomass was dried and kept at 4 °C. Experimental compounds used included methanol, trichloromethane (>99%), methyl pentadecanoate (>98%), sulfuric acid (98%), n-hexane (97%), and malonic acid (Shanghai Aladdin Biotechnological Co., Ltd., Shanghai, China). Choline chloride and n-butanol (Shanghai Macklin Biochemical Co., Ltd., Shanghai, China) Ethyl acetate (99.8%) were purchased from Sigma-Aldrich (Shanghai, China) Trading Co., Ltd.; formic acid and acetic acid were also purchased (Macklin, Beijing Minda Technology Co., Ltd., Beijing, China).

Surfactants such as N-Hexadecyl trimethylammonium chloride (HTAC), with purity greater than 99%, were purchased from Aladdin Industrial Corporation, Shanghai, China. Fatty alcohol polyoxy-ethylene ether (JFC) was purchased from Wuhan Oxiran Specialty Chemicals Co., Ltd., Wuhan, China. Coconut glucoside (APG 0814) and Lauryl glucoside (APG 1214) were provided by Yangzhou Guanmin Imp. & Exp. Co., Ltd., Yangzhou, China. When strictly necessary, ultrapure water was used.

2.2. Solvent Preparation and Analysis

Surfactant solutions were prepared by mixing surfactants (in powder or liquid state) at different concentrations with deionized water until total homogeneity according to the procedure reported in [15].

The various types of hydrogen bond donors used in this study for biomass pretreatment were selected based on prior studies in which deep eutectic solvents were employed for pretreatment in order to recover a compound from a biomass [11,16]. Choline chloride was heated with hydrogen bond donors at various molar ratios, resulting in the formation of eutectic solvents. In this experiment, acetic acid, malonic acid, and formic acid were used as hydrogen donors, and choline chloride served as a salt. The mixture was heated to 80 °C and stirred vigorously for 120 min with a magnetic stirrer at a speed of $\leq$8000 rpm until a transparent, uniform liquid was produced [17]. To prevent external water absorption, the produced DES was sealed and kept in a desiccator. The other deep eutectic solvent, which was not developed in this study, was not stable at room temperature (25 °C).

FTIR analysis confirmed the formation of DESs. The components used in this study for the synthesis of deep eutectic solvents are listed in Table 1.

Table 1. Molar ratio and the density value of DESs' selected.

Organic Salts	Hydrogen Bond Donor	DES Molar Ratio	Density ρ, (g·mL^{-1})
Choline chloride	Malonic acid	1:1	1.08
Choline chloride	Formic acid	1:3	1.12
Choline chloride	Acetic acid	1:3	1.02

DESs' structures were optimized using the Gaussian 09 suite of programs [18] at the DFT/B3LYP/6-311G(d,p) level of theory [19]. Grimme's type dispersion corrections (GD3) were incorporated into the function to obtain a deep description of weak interactions [20]. Topological analysis was thus performed on the molecular complexes formed between the ChCl.MA DES and cellulose to further highlight the interactions leading to the disruption of the cell wall in the pretreatment step. This was performed using the Bader's approach and via the multiwfn program package.

2.3. Pretreatment of Microalgae Biomass

Firstly, the total lipid content of our biomass was determined according to the conventional modified Folch's method [21]. According to some studies, surfactants were used to ease the disruption of the algae cell wall and enhance the lipid yield [22,23]. Aside from its role in facilitating microalgae cell disruption, surfactants have been proven to be viable alternatives to some environmentally toxic organic solvents [7].

Based on the above-mentioned studies, the effects of different surfactants (HTAC, JFC, APG0814, and APG1214) were tested to investigate their influence on lipid extraction. In summary, 0.2 g of dried biomass was mixed with 3 mL of n-butanol/ethyl acetate at a ratio of 1:2 and 2 mL (0.5% dosage of each surfactant), sonicated for 10 min, and then centrifuged at 4000× *g*. To separate the lipid from the water and residuals, the lipid layer collected into a pre-weighted round flask was subjected to solvent removal using a rotary evaporator (RE-501, Zhengzhou Haiqi Instrument Technology, Zhengzhou, China). For the blank sample test, 2 mL of n-hexane was added to extract the lipid. The following formula, which had been previously employed by Lu et al. [24], was used to calculate the lipid yield, which was determined gravimetrically:

$$Lipid\ yield\ (\%) = \frac{Weight\ of\ lipid\ extracted\ from\ the\ dried\ biomass\ (mg)}{Weight\ of\ the\ dried\ biomass\ (mg)} \times 100 \quad (1)$$

According to Loos and Meindl [25], the cell wall components of *Chlorella* sp. are typically cellulose, hemicellulose, protein, lipid, and ash. Therefore, the cellulose and hemicellulose in the cell walls of the microalga *Chlorella* sp. are likely to be affected by the hydrogen bonds between hydroxyl, anions, carboxyl, or acylaminoin aqueous DESs and hydroxyl composing the cell wall, resulting in an increment in the amount of lipid extracted due to cell wall modification. Based on this knowledge, an experiment involving biomass pretreatment with a deep eutectic solvent was performed in order to improve the cell-breaking process and thus increase lipid extraction. The experiment investigated the usage of three DESs in order to identify the best for pretreatment, including ChCl:AA (1:3), ChCl:FA (1:3), and ChCl:MA (1:1).

For this purpose, 0.2 g of *Chlorella* microalgae powder was mixed with 4 g of each DES (ChCl:AA (1:3), ChCl:FA (1:3), and ChCl: MA (1:1)). The biomass was washed several times with distilled water. Centrifugation (at 8000 rpm for 10 min) was used to separate water and biomass; then, biomass was recovered and dried in a vacuum oven for 12 h at 50 °C (Model: BOV-30V from Biobase Meihua Trading Co., Ltd., Jinan, China; thermogravimetric analysis (TGA) model from NETZSCH (Selb, Germany). Scanning Electron Microscopy (SEM) was used to investigate the conformation of biomass as a result of DES pretreatment. The lipid was collected to assess the various DESs involved in the pretreatment step, following a procedure similar to that described above.

2.4. Total Lipid Content and Optimization of the Lipid Extraction Process

A conventional Folch's methol [21] was employed for total lipid content determination of biomass to compare its efficiency with that of the new analysis method. In brief, 0.2 g of dried biomass and 5 mL of chloroform/methanol (2:1) were used for lipid extraction, with continuous stirring applied for 30 min at room temperature and the addition of 8 mL Milli-Q water. After that, the sample was centrifuged for 10 min at 3500× *g*, and the bottom layer (chloroform containing lipids) was removed and transferred to a pre-weighed vial. The above protocol was repeated two times on the residual biomass, and the supernatant was combined. The pre-weighed vial containing supernatant was dried using a rotary evaporator before being weighed with a microbalance to determine the lipid content.

Through the single-factor experiment, several variables were explored in order to establish the best lipid extraction conditions for the DES-pretreated biomass. An n-butanol/ethyl acetate combination was used as a solvent, for which variables such as time (30, 60, 90, 120, and 150 min), temperature (40, 50, 70, and 80 °C), n-butanol/ethyl acetate ratios (1:0, 1:1, 1:2, 1:3, 1:4, 1:5, 1:6, and 0:1 *v*/*v*), and concentration of the surfactant (0.1, 0.2, 0.3, 0.4, 0.5, 0.6, 0.8, 1, 1.2, and 1.4%) were analyzed (as shown in Figure 1).

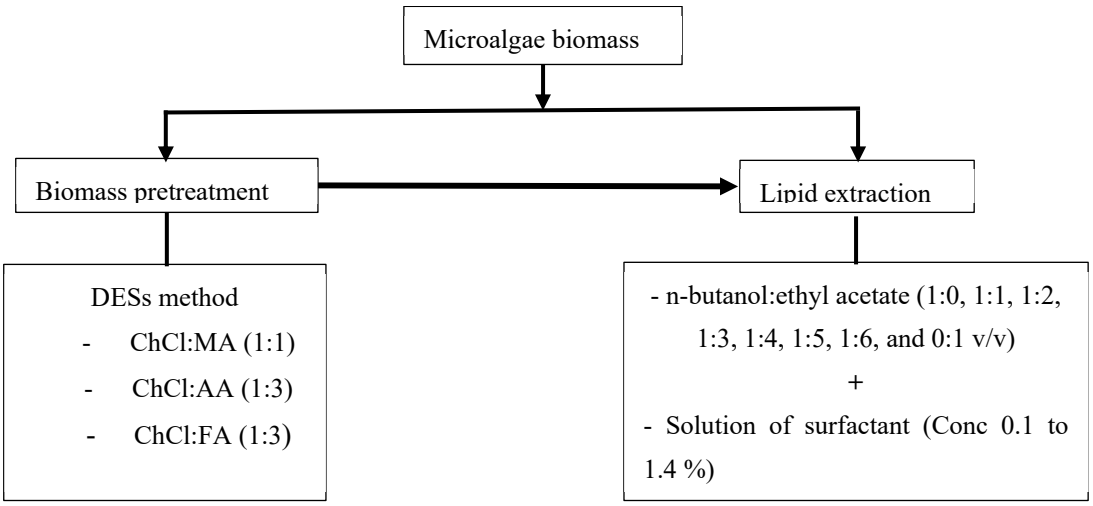

Figure 1. Flowchart of lipid extraction from pretreated microalgae.

For lipid extraction, in a 10 mL volumetric sealed flask, 0.2 g of pretreated biomass, 3 mL of n-butanol/ethyl acetate, and 2 mL of surfactant solution were thoroughly agitated and placed under ultrasonic treatment (VEVOR Ultrasonic Cleaner). The mixture was then placed in a centrifuge tube and centrifuged after being washed with 10 mL of distilled water (4000× *g* for 10 min in an 800-1 Centrifugal machine) to separate the lipids from the water and residuals. Lipid yield was determined gravimetrically as a percentage of the dry weight of the microalgal biomass and calculated using Equation (1).

2.5. Fatty Acid Methyl Ester Profile and Biodiesel Analysis

The extracted lipids, under optimum conditions, were transesterified according to the procedure reported by Lu et al. [24]. A volume of approximately 0.0017 g of lipids was deposited into a glass tube and transesterifed with 2% H_2SO_4 as a catalyst at 80 °C for 2 h 30 min via magnetic stirring. The mixture was then allowed to cool at room temperature for 20 min. Subsequently, a 10:1 lipid-to-hexane ratio was added to extract the FAME, and the mixture was vortexed for 30 s and centrifuged at 3500× *g* for 5 min to form a binary phase. The upper phase, which was rich in FAMEs, was filtered, transferred to a clean bottle, and then dried under a rotary evaporator. FAMEs were analyzed according to the procedure reported in [24].

Gas chromatography–mass spectrometry (GC–MS) analysis was conducted using an Agilent USA 8890 GC system and an Agilent USA 7000 DGC/TQ system equipped with a

30 m 0.25 mm i.d. capillary column with 0.5 µm film thickness (HP-5MS) (Agilent, Santa Clara, CA, USA, Serial No.: T562436H) and an auto sampler. Methyl pentadecanoate was used as standard for the FAME analysis. The key characteristics of biodiesel were examined using the Biodiesel analyzer V 1.1 software (http://www.brteam.ir/biodieselanalyzer) [26] (accessed on 19 April 2023), including cetane number (CN), iodine value (IV), degree of unsaturation (DU), saponification value (SV), kinematic viscosity (KV), oxidative stability (OS), content of saturated fatty acids (SFA), and higher heating value (HHV). This software has been used to estimate the properties of biodiesel made from a microalgae and yeast co-culture [27].

2.6. Analytical Examination

An FTIR WQF-520 FTIR spectrometer equipped with DTGS and MCT detectors and running FTIR software (Beijing Rayleigh Analytical, Beijing, China) was used to analyze biomass, both untreated and pretreated, in the 4000–500 cm^{-1} range.

Thermogravimetric analysis (TGA) was used to determine the thermal behavior of microalgae using a TGA analyzer from NETZSCH, Germany, and an inert atmosphere with a 20 mL/min velocity. To perform the analysis, 0.01 g of algal biomass was heated from 20 to 900 °C in a ceramic crucible.

The configuration of both the untreated and treated microalgae biomass was performed via SEM (SU8010, Hitachi, Tokyo, Japan) to determine whether there were any modifications during the treatment. A 10,000× magnification level was used for the test, which was applied to 25 mm aluminum stubs to which a double-sided conductive adhesive that was initially gold-sprayed had been applied. At room temperature, the densities of the produced DESs were determined gravimetrically. A 1 mL pipette was used to calibrate the electronic scale, and 1 mL of each DES was transferred into the vial before measurement. The liquid volume mass was then calculated.

2.7. Statistical Examination

The average values and standard deviations of all the experiments, which were performed more than once, are presented as the final results. When necessary, analysis of variance (ANOVA) was employed during data analysis using Origin Pro 8.6 (Origin Lab, Northampton, WA, USA) and Excel 2003 (Microsoft Office Enterprise).

3. Results and Discussion

3.1. FTIR Analysis of Synthetized Deep Eutectic Solvents

Three types of DESs based on ChCl and carboxylic acids were synthesized at different ratios: choline chloride—formic acid at (1:1), (1:2), and (1:3) ratios; acetic acid at (1:1), (1:2), and (1:3) ratios; and malonic acid (ChCl:MA) at ratios (1:1), (1:2), and (1:3). Among the DESs synthesized, only the ratios ChCl:FA (1:3), ChCl:AA (1:3), and ChCl:MA (1:1) were chosen for the next experiments because the other ratios were found to be unstable (they solidified at room temperature). Their structures were probed using a FTIR study. Figure 2 illustrates the chemical-bonding patterns of the precursors (choline chloride and the respective hydrogen bond acceptors (HBAs)) and their combinations.

Figure 2b presents very broad bands in the range from 3500 to 1000 cm^{-1} in the DES (ChCl:FA) related to C-O stretching, O-H stretching, C-H stretching, and sp^3 C-O stretching vibrations, which were attributed to bands at 3330, 2920, 2650, 1720, and 1080 cm^{-1}, respectively (C-O stretching in ChCl). As new hydrogen bonds were formed, the O-H vibration frequency at 3027 cm^{-1} in ChCl reduced to 2920 cm^{-1} in formic acid. Figure 2a,c show that a difference in the vibrational bands, a property of tertiary amine salts, was detected via FTIR in the mixture of ChCl and AA and that of ChCl and MA. ChCl fluctuates between 2500 and 2000 cm^{-1}. O-H bond stretching was confirmed via the presence of a bandwidth between 3200 and 2500 cm^{-1}. These spectra (ChCl:AA) support the production of DES and suggest the presence of hydrogen-bonded carboxylic acids (carboxylic acid dimers) or molecules of carboxylic acid.

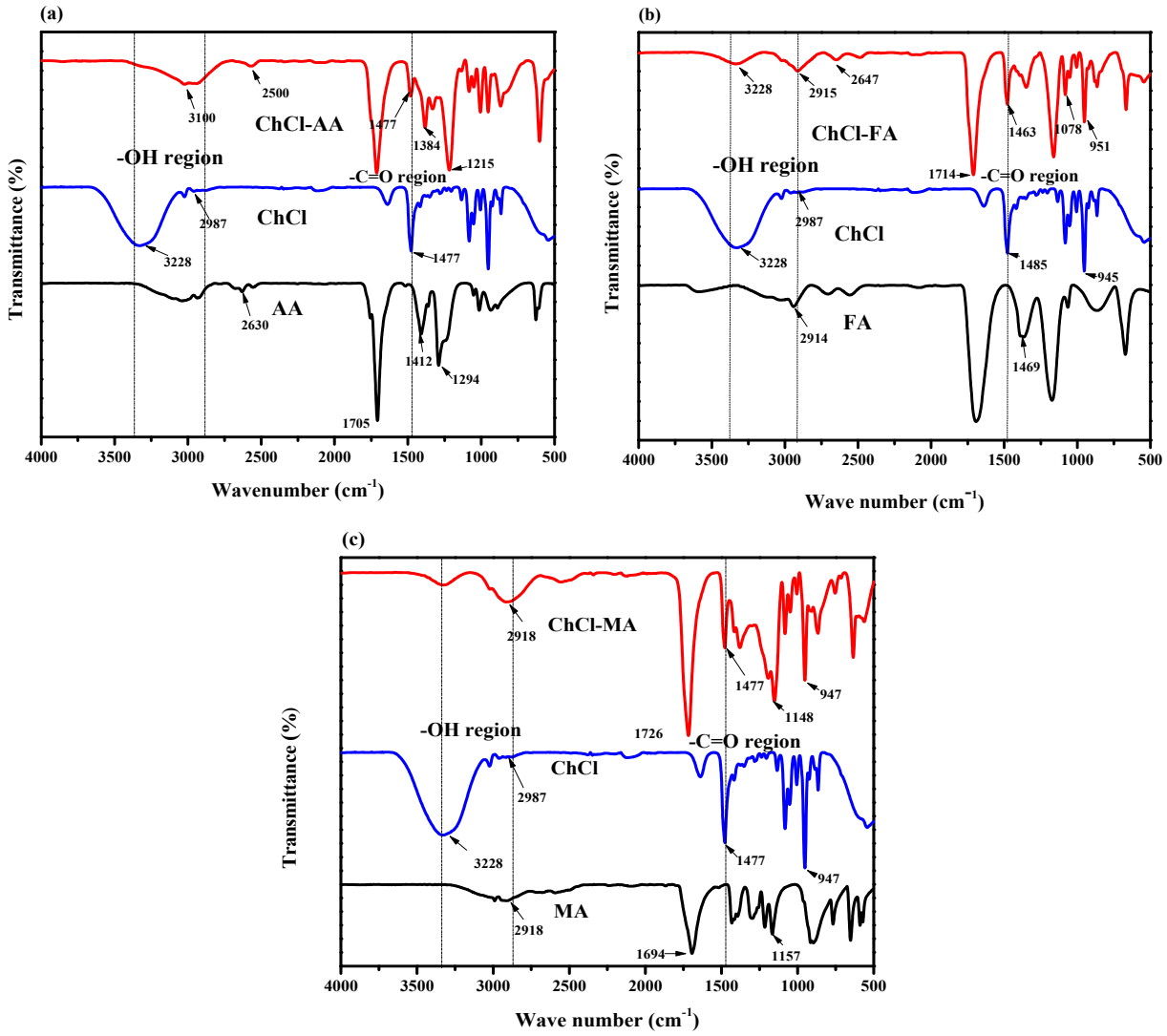

Figure 2. FTIR spectra of the DESs: (**a**) ChCl:AA, (**b**) ChCl:FA, and (**c**) ChCl:MA.

The density of a solvent affects its mass flow and ability to permeate or penetrate the cell membrane. The density value was ≈1 g·mL^{-1} for all the DESs prepared in this investigation. The DES ChCl:FA was found to have the highest density value (1.12) among the three DESs, as shown in Table 1. This result is highly related to the nature of HBD and the dynamics of interaction during the reaction. The difference observed in the values could be explained by the length of the alkyl chain. The density of a DES is inversely proportional to the increase in length of the alkyl chain, whereas the equivalent molar volume rises according to the same trend [28].

3.2. Geometric Optimization of DESs' Structures

Figure 3a–c show the theoretically relaxed structures of the DESs ChCl:FA (1:3), ChCl:AA (1:3), and ChCl:MA (1:1). The structures of these DESs show evidence of several hydrogen bonds (HB). The lengths of the C-H . . . Cl non-conventional HBs found in their structures were observed to be between 2.64 and 2.78 and between 2.64 and 2.80 Å for the DESs ChCl:FA (1:3) and ChCl:AA (1:3), respectively. Concerning ChCl:MA (1:1), the length of its C-H . . . Cl bond is in the range 2.71–3.02 Å. These values are higher than those obtained when using the same theoretical chemistry method for the relaxed structure of free ChCl (2.37–2.46). The increment in the C-H . . . Cl bond length observed is due to the presence of carboxylic acids. Indeed, some of the lone electrons of the Cl-atom are used by the ChCl moiety to link the acetic acid molecules through conventional O-H . . .

O HBs. The lengths of the HBs ranged from 2.15–3.04, 2.03–2.14, and 2.02–2.71 Å for the DESs ChCl:FA (1:3), ChCl:AA (1:3), and ChCl.MA (1:1), respectively. Mulliken's atomic charge of the Cl-atom in the free ChCl structure was found to be −0.802 a.u. This charge was found to be less negative in the presence of carboxylic acids, with values of −0.702, −0.693, and −0.733 a.u. in ChCl:FA (1:3), ChCl:AA (1:3), and ChCl:MA (1:1), respectively. Consequently, the basicity of the Cl-atom of ChCl reduces in carboxylic acid solutions.

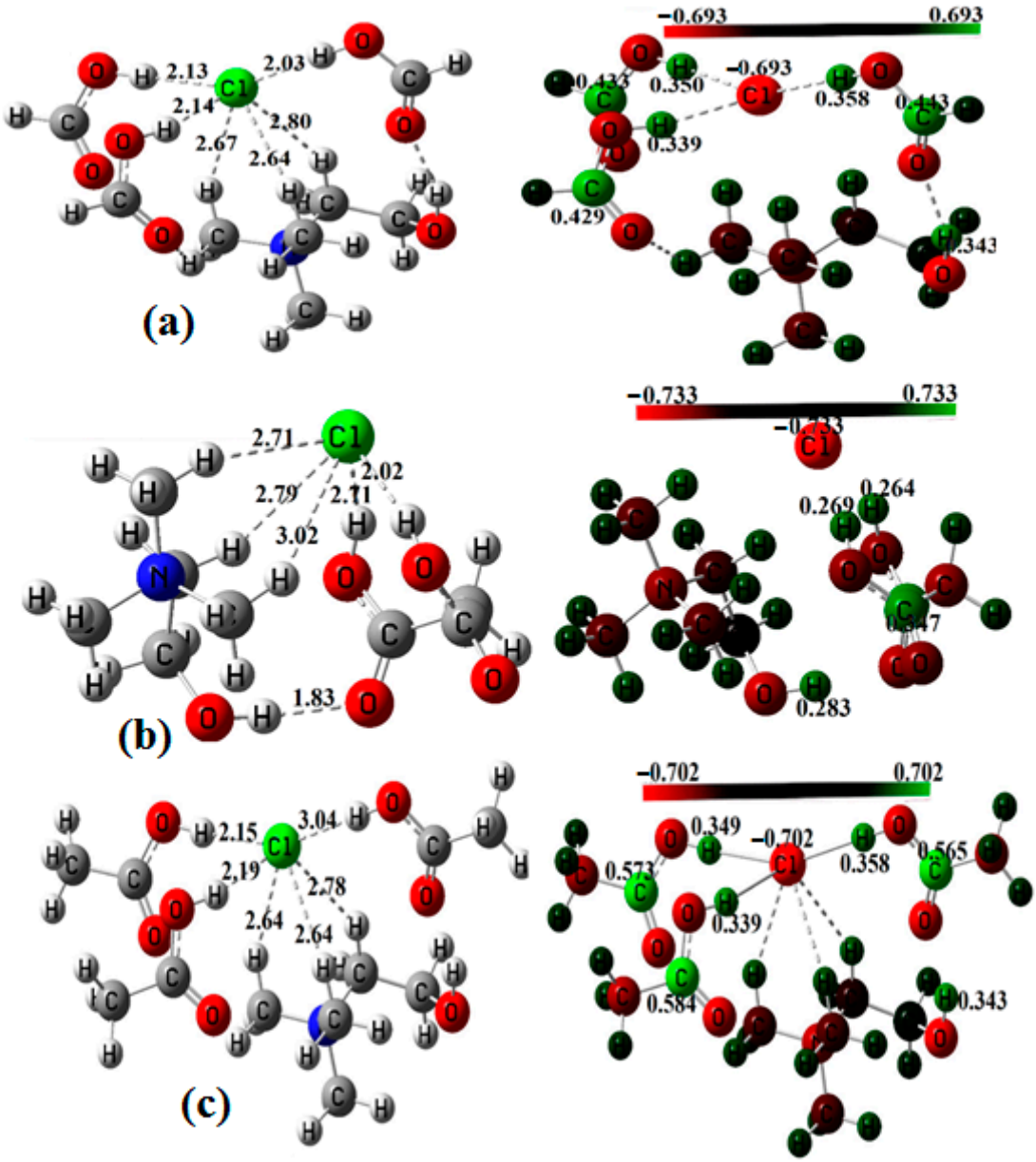

Figure 3. Optimized structures of DESs used. The Mulliken's atomic charges of some atoms and their structure obtained at the DFT/B3LYP-D3/6-311G(d,p) level of theory. (**a**) ChCl:MA (1:1), (**b**) ChCl:AA (1:3), and (**c**) ChCl:FA (1:3).

Acidic conditions promote the degradation of the cell walls of microalgae and improve lipid extraction [29]. An analysis of the non-covalent interactions of these DESs based on the reduced diagram method yielded the results presented in Figure 4. Indeed, the use of the non-covalent interaction (NCI) method, which is also known as the reduced density gradient (RDG) method, is very popular for studying weak interactions. The NCI method makes it easier to characterize weak interactions such as van der Waals (VDW) forces, dihydrogen bonds, π-stacking interactions, and halogen bonds. These interactions play

crucial roles in terms of structures, reactivity, and selectivity and in the physical, chemical, and biological properties of molecular systems. The NCI index also has the advantage that it permits the visualization of weak interactions in real space by means of 3D isosurfaces. From the color-filled RDG isosurfaces, different types of regions can be identified by simply examining their colors. The color scale bar presented in Figure 4 shows that the blue-colored isosurfaces indicate stronger attractive interactions, such as strong HBs, whereas attractive VDW forces are depicted by the greenish or blueish surfaces [30,31].

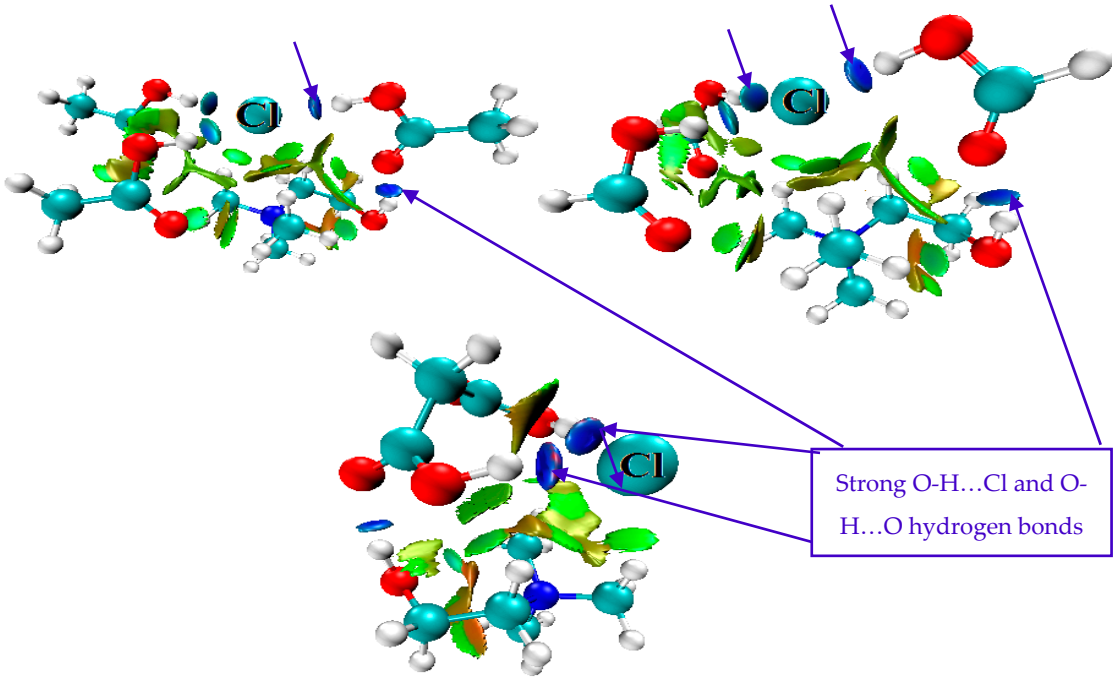

Figure 4. Labeled 3D diagram of non-covalent interactions on the isosurfaces of the DESs studied, showing blue (OH … Cl and O-H … O hydrogen bonds) and green (attractive van der Waals interactions) isosurfaces between the ChCl and the carboxylic acid moieties.

Figure 4 reveals the presence of strong hydrogen bonds depicted by the blue disc-like surfaces between O-H groups (from the acetic acid) and Cl-atoms (of ChCl) and between the O-H from the ChCl moiety and the carboxylic O-atom, as previously mentioned between the ChCl and the carboxylic acid moieties. The interaction regions marked by green circles can be identified as the vdW interaction region because the mapped color is green or light brown, which shows that the electron density in these regions is low. These vdW interactions occur due to attractive forces between the alkyl H-atoms and Cl as well as the O-atoms of the carboxylic acids. They greatly contribute to stabilizing the molecular systems of DESs. These observations show that both ChCl and carboxylic acids can strongly link to compounds containing polar groups (such as –OH groups) such as cellulose and lignin, thus facilitating the extraction of like compounds from microalgae.

3.3. Surfactant Screening

Surfactants are functional materials with unique features that can affect lipid–water interfacial properties. Firstly, the total lipid content of our biomass was ascertained to be 17.21% using the conventional modified Folch's method. This study compared two classes of surfactants (Table 2). N-Hexadecyl trimethylammonium chloride (HTAC), fatty alcohol polyoxy-ethylene ether (JFC), coconut glucoside (APG 0814), and lauryl glucoside (APG 1214) are some of the most often-utilized surfactants.

Table 2. Surfactants used and their critical micellar concentrations (CMCs).

Type	Surfactants	CMC [(a)] (mM) at 296.15 K–248.15 K
Cation	N-Hexadecyl trimethylammonium chloride (HTAC)	0.94–1.19 [32]
Non-ionic	Fatty alcohol polyoxy-ethylene ether (JFC)	0.019 [33]
	Coconut glucoside (APG 0814)	0.13 [34]
	Lauryl glucoside (APG 1214)	0.13 [35]

[(a)] Critical Micellar Concentration.

Figure 5 summarizes how the surfactants improved lipid recovery when the n-butanol/ethyl acetate solvent was added. Most of the surfactant-treated samples were found to exhibit better lipid recoveries than the control biomass, in which hexane was used as a co-solvent to extract lipids. A lower lipid yield of 3.45% was obtained from the control biomass when compared to those using surfactants (wherein HTAC > APG0418 > JFC > APG1214). HTAC yielded the highest value: 8.725%. The use of surfactants facilitates the disruption of the algal cell wall and enhances lipid yields [36]. Moreover, the presence of surfactants has been shown to improve lipid extraction yields. Additionally, they were reported to be suitable alternatives to organic solvents in the lipid extraction processes [7]. Surfactants are made up of a hydrophilic group and a hydrophobic group. The hydrophilic group can be adsorbed at the surface of the lipid droplet, while the lipophilic group can be inserted into the droplet [37]. A surfactant's functional components are involved in the interactions with the lipid phase and water phase. Surfactants can cause the lipid–water phase to appear as a layered structure by lowering the surface tension and surface free energy in this system [38]. Consequently, this reduces the interaction of lipids with cell tissues. During the homogenization process, mechanical forces strip the lipid-like substance from the cell tissues. On the fresh surface created via the stripping procedure, surfactant molecules are adsorbed. Ultimately, the lipids will separate entirely from the cellular structures and diffuse into the solvent medium.

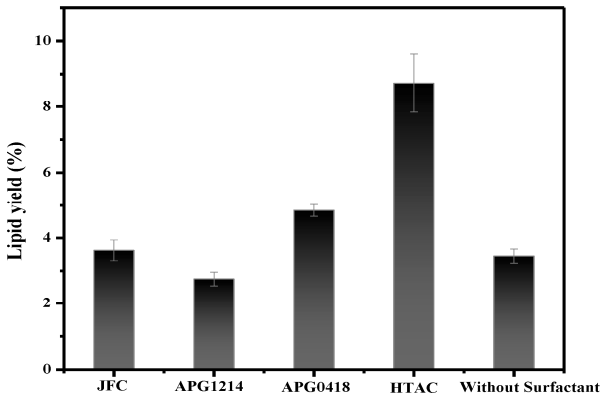

Figure 5. Lipid yield from biomass pretreated by n-butanol/ethyl acetate and using different surfactants as co-solvent.

Moreover, as shown in Figure 5, the surfactant HTAC leads to a better lipid yield value of 8.725% compared to the other surfactants. This result might be attributed to the superior solubility of cationic surfactants such as HTAC. Some studies have mentioned that cation surfactants performed better than any other type of surfactant. This is due to the fact that cationic surfactants can easily bind to microalgae membranes and cause effective cell disruption [39].

3.4. DESs Effect on Biomass Pretreatment

Since most algae have a rigid and intricate cell wall, it is necessary to break down the microalgal cell wall in order to extract lipid and other microalgal compounds from microalgal biomass. Three different DESs, ChCl:MA (1:1), ChCl:FA (1:3), and ChCl:AA (1:3), were used in this study to pretreat *C. pyrenoidosa* biomass for lipid extraction. The lipid yields of various DES-pretreated biomass are shown in Figure 6. Almost all the DESs tested showed an acceptable lipid yield, with values of 12.365%, 9.15%, and 11.08% obtained for ChCh:MA, ChCl:FA, and ChCl:AA, respectively. According to a study by Loos et al., hemicellulose, cellulose, lipids, proteins, and ash are the main components of the cell walls of different species of *Chlorella* [25].

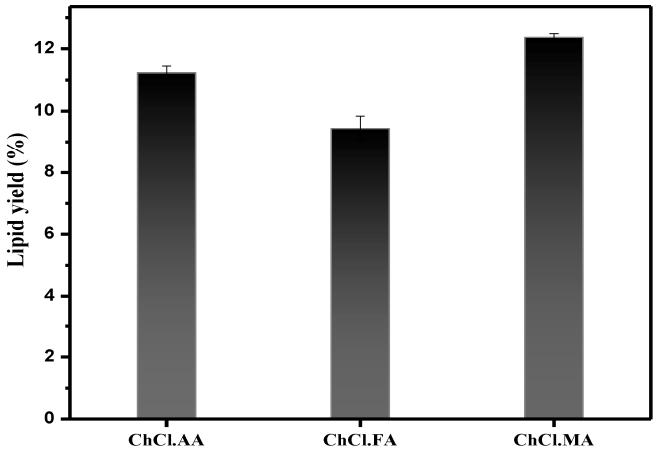

Figure 6. The lipid yields of various DES-pretreated biomasses.

As a result, it is predicted that hydrogen bond formation between anions, hydroxyl groups, carboxyl groups, or acylamino groups in the aqueous DES and hydroxyl in the cell membrane might potentially alter the hydrogen bonds of cellulose and hemicellulose in the cell walls of microalgal *Chlorella* sp. [11].

3.5. Characterization of Microalgae

3.5.1. SEM Analysis of the Biomass

Since most algae have a rigid and intricate cell wall, it is necessary to break down the microalgal cell wall in order to extract biocomposites from the microalgal biomass. Figure 7a,b show macroscopic images of the microalgae before and after DES treatment. Electronic microscopy was used to deeply analyze the structures of the cell membranes before and after the pretreatment. The difference in the configuration and the morphology can be clearly observed. A round and well-defined cell membrane from the control biomass changes to a dimorphic and irregular morphology after DES ChCl:MA-pretreatment, as shown in Figure 8.

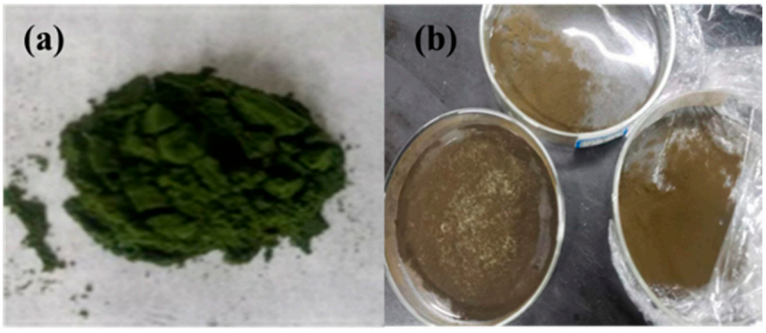

Figure 7. Microalgae powder: (**a**) unpretreated and (**b**) DES-pretreated biomass.

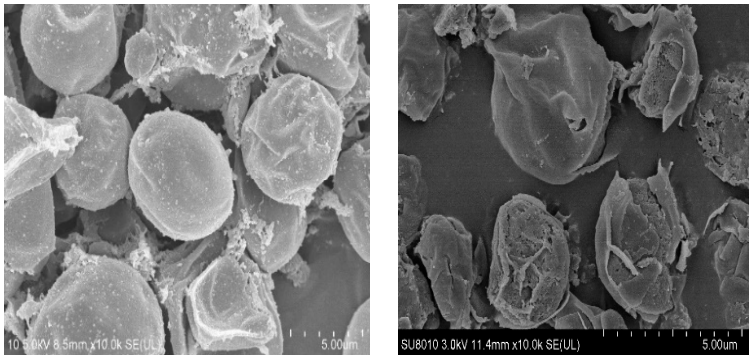

(**a**) (**b**)

Figure 8. SEM images of the biomasses' cell surfaces (**a**) before and (**b**) after DES pre-treatment.

3.5.2. Thermogravimetric Analysis of the Biomass

Figure 9 displays the results of the thermal analysis of the untreated and treated microalgae biomass. The following temperature ranges determine the three phases of the thermal degradation of the microalgal biomass: dehydration occurs when volatile compounds and moisture are lost between 40 and 165 °C; devolatilization occurs between 165 and 450 °C when major compounds such as carbohydrates, lipids, and proteins are broken down; and solid disintegration occurs between 450 and 898 °C when biochar is formed [40]. As seen in Figure 9, due to water loss, a peak in the temperature of the non-pretreated and pretreated biomass is observed in the first phase at approximately 47.28 °C and 47.84 °C, respectively. After the pretreatment, the observed minor increase in the peak could be due to the fact that the pretreatment significantly improves the disintegration of the cell wall, leading to the alteration and thermal expansion of biomolecular structures [41].

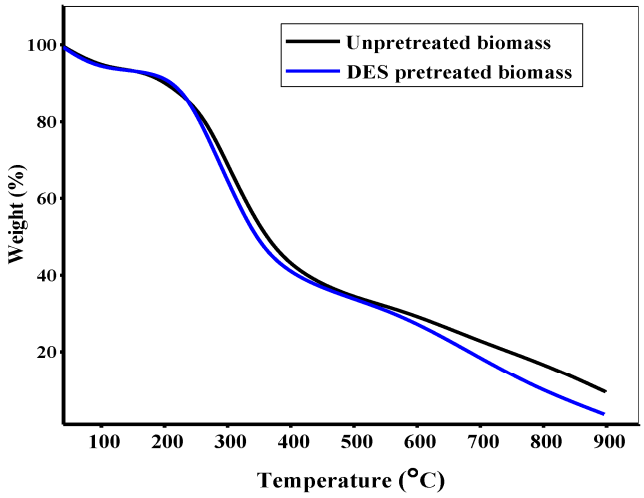

Figure 9. TGA curve of *Chlorella* sp. biomass.

3.6. Mechanism of Cell Wall Disruption Inflicted by DES

The evaluation of the events that transpired throughout the pretreatment process required a thorough understanding of the mechanisms underlying the cell disruption caused by DES. Typically, microalgae with cellulose- and/or hemicellulose-based cell walls are more resistant to damage [42]. Cell wall components such as cellulose, which interact with DES, may constitute the underlying mechanism behind the degradation of cell walls. Therefore, it is interesting to learn more about the chemical mechanisms behind cellulose's interaction with DES species. A significant part of the disruption of cellulose is engendered by DES species. To further highlight this interaction, DFT simulations of the mechanisms occurring between cellulose and the DES choline chloride/malonic acid (1:1) in the pretreatment (1:1) were performed.

Accordingly, the cellulose–ChCl.MA molecular complexes were allowed to relax at the B3LYP-D3/6-311G(d,p) level of theory in a gas phase. Cellobiose was utilized as a model molecule since the structure of cellulose consists of 100,000 (1–4) connected D-glucose units. Furthermore, frequency calculations on the relaxed geometries showed that there was no imaginary frequency, indicating that the structures correspond to the actual minima of the potential energy surface. Identifying the non-covalent interactions between cellobiose and DESs is the key goal in this regard. Thus, the Quantum Theory of Atoms in Molecules (QTAIM) [43] and reduced density gradient (RDG) [44] methods were applied. Figure 10 shows the resulting molecular diagram of cellulose and ChCl.MA.

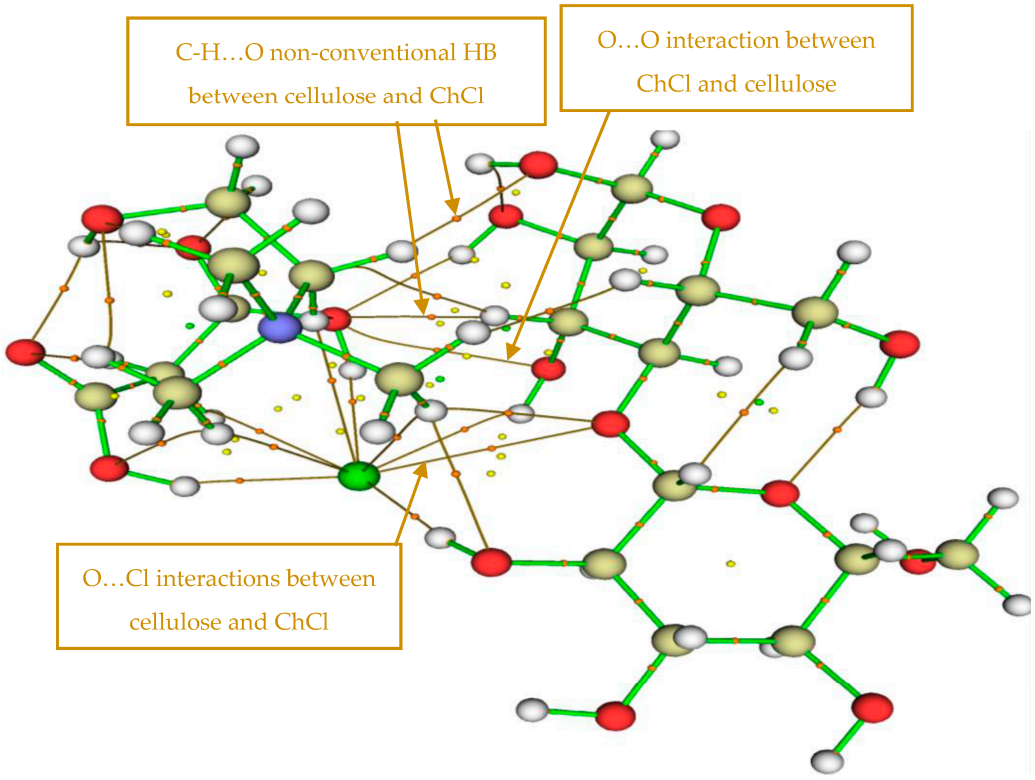

Figure 10. Molecular graphs of the cellulose–ChCl:MA molecular complex. The green lines represent covalent bonds, the orange lines are bond paths, and the orange, yellow, and green spheres correspond to the critical points of bonds, rings, and cages, respectively.

It can be observed in Figure 11 that several NCIs stabilized the cellulose and ChCl.MA complex, the strongest of them being O-H . . . Cl HB. Indeed, two O-H . . . Cl HBs were identified in that structure and confirmed via analysis of their RDG isosurfaces. Figure 11 also shows that one of these HBs is characterized by a greenish RDG isosurface, while the second has an obviously green isosurface (See Figure 10), showing a great difference in their strength. The energy (E_{HB}) of these HBs (−3.93 and −2.09 kcal/mol) clearly corroborates the difference observed in their strengths. Moreover, two non-conventional C-H . . . O HBs involving the aliphatic C-H groups of the ChCl moiety and the O-atom of the hydroxyl groups of cellobiose, with E_{HB} values of −1.96 and 2.02 kcal/mol, were found. A similar interaction involving a C-H aliphatic group of ChCl and the O-atom linking the cycles of cellobiose was found, with an energy value of −1.46 kcal/mol. In addition to the above-mentioned interactions, interesting O . . . O-, H . . . H-, and O . . . Cl- attractive NCIs were found between the cellobiose and DES moieties, with respective energy values of −1.88, 1.39, and 1.00 kcal/mol. The RDG analysis confirmed that all of the latter values corresponded to attractive van der Waals interactions. The HB and VDW interactions observed between the DESs and cellobiose weaken the cell membrane of microalgae in the pretreatment step and, subsequently, ease the extraction of the compound.

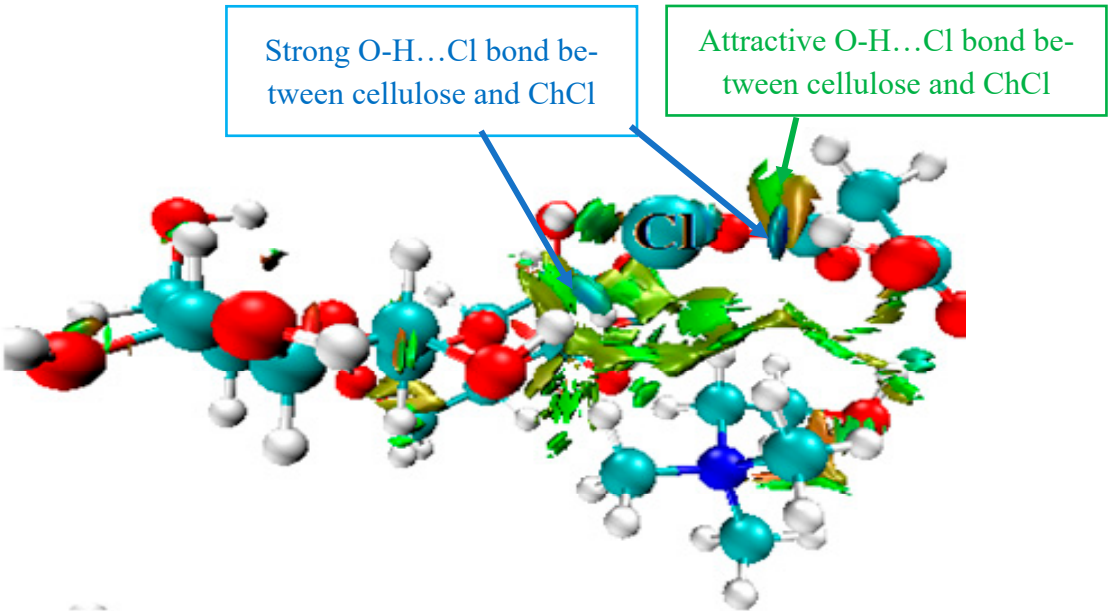

Figure 11. Labeled 3D NCI isosurfaces of the cellulose–ChCl.MA molecular complexes.

3.7. Optimization of Lipid Extraction Process Using Single-Factor Experiment

3.7.1. Effect Temperature on Lipid Extraction

Temperature has been demonstrated to be an important parameter of lipid extraction. The temperatures selected for extraction were 30, 40, 50, 60, 70, and 80 °C. According to the ultrasonication settings, the final temperature was set at 80 °C and did not rise above 80 °C. Other conditions were set, as follows: extraction time—30 min; amount of solvent used—3 mL (n-butanol to ethyl acetate ratio—1:2); and HTAC percentage—0.5%. The biomass-to-solvent volume was fixed at 3 mL during the whole experiment because the use of more solvent can be dangerous for the environment [24].

Lipid yield increased steadily with the increase in temperature and reached a maximal value of 15.25% at 80 °C. However, it was predicted that, after 80 °C, the lipid yield would decrease (Figure 12a). According to Shi et al., a high temperature may cause the softening of plant tissue, disrupting the interactions between phenolic compounds and lipids, proteins, or polysaccharides and increasing the rate of diffusion, thus enabling a higher rate of extraction [45]. The boiling point of the solvent and the fact that it evaporates might also induce a discrepancy in the lipid yield [10]. Previous research [24] found similar tendencies, wherein a temperature of 80 °C was identified as ideal.

3.7.2. Effect of Time on Lipid Extraction

The experiment on the effect of extraction time on lipid yield was carried out under standard conditions (a n-butanol to ethyl acetate ratio of 1:2, a temperature of 80 °C, and an HTAC solution concentration of 0.5%). Figure 12b shows that the lipid yield increased from 14.725% to 15.9% when the extraction time increased from 10 to 60 min. This result can be attributed to the fact that it takes time for a solute to easily penetrate, dissolve lipids, and disperse a decomposer out of the cells. The recovery yield of lipids remained approximately the same when the time was extended to 90 min. The recovery efficiency of the lipids decreased slightly when the extraction time was prolonged beyond 60 min. To avoid wasting time on this experiment, 60 min was chosen as the best time span. Moreover, previous research revealed that longer reaction times can reduce the phenolic activity required for lipid synthesis [24].

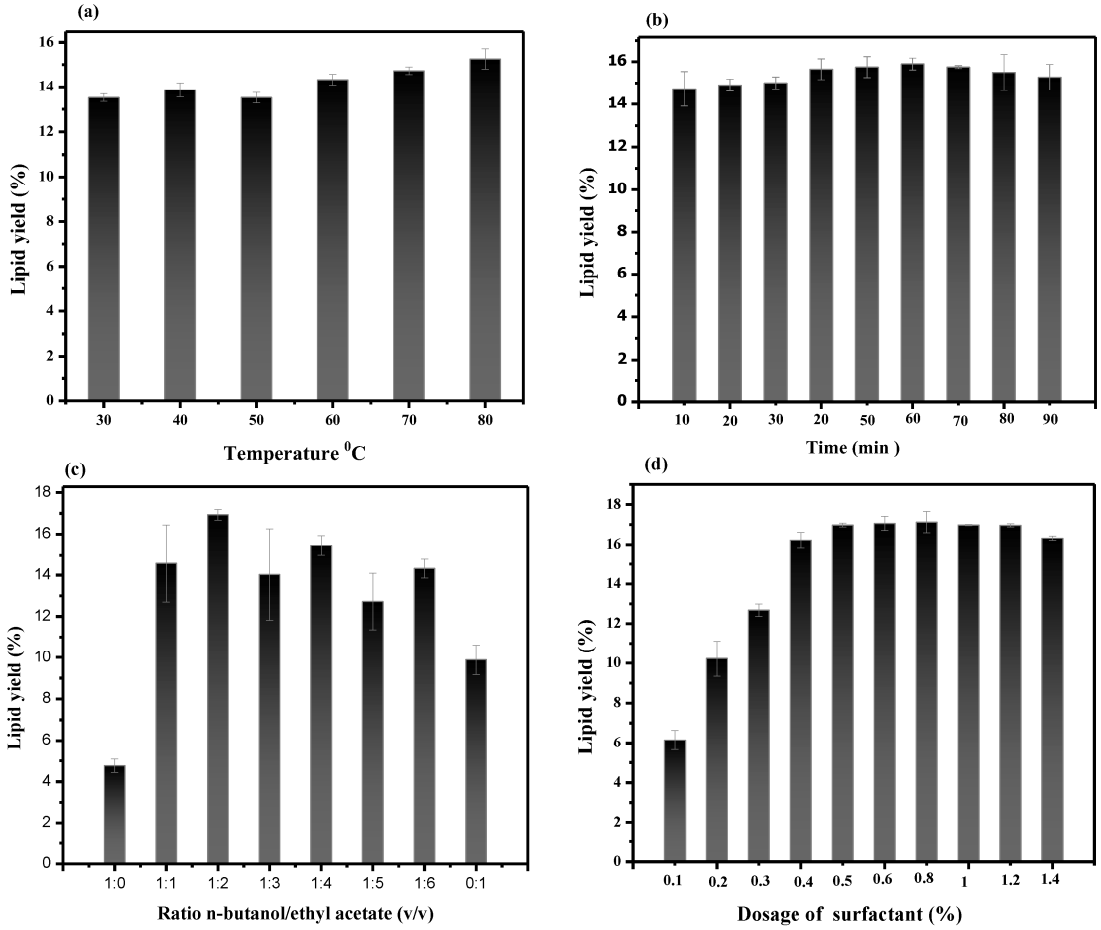

Figure 12. Influence of different variables on lipid yield: (**a**) temperature, (**b**) time, (**c**) ratio of n-butanol to ethyl acetate (v/v), and (**d**) dosage of surfactant.

3.7.3. Effect of n-Butanol-to-Ethyl-Acetate Ratio on Lipid Extraction Yield

The yield of lipid extraction is significantly influenced by both the permeability of cell walls and the solubility of lipids in solvents. A previous study, ref. [46], showed that using both polar and non-polar solvents together can increase the amount of lipids that can be extracted compared to using either solvent alone. Additionally, it was reported that solvent–lipid interaction may occur when the Hildebrand solubility parameters (HSP) values of the solvent's and microalgae's lipids are in close proximity [24]. Oil-like molecules have were determined to have an HSP value of 17.5 in this study.

n-butanol and ethyl acetate have HSP values of 16.0 and 18.2, respectively [47]. Butanol is significantly more soluble in lipids than ethyl acetate, although ethyl acetate has a far higher solubility in neutral lipids. Thus, in order to understand the efficacy of lipid extraction, the effects induced by n-butanol/ethyl acetate ratios of 1:0, 1:1, 1:2, 1:3, 1:4, 1:5, 1:6, and 0:1 were tested in this experiment.

The highest yields (16.93%) were obtained when the n-butanol/ethyl acetate ratio was 1:2. At a volume ratio of 1:2 (v/v), the mixed solvent was more capable of penetrating the cell membrane and entering the cytoplasm, where it can interact with the lipid complex. Figure 12c shows that the results are much higher than those obtained when either n-butanol (4.76%) or ethyl acetate (9.88%) were used alone. This suggests that a certain mixture of solvents is more appropriate to extraction than a single solvent. The lipid yield was reduced when the n-butanol/ethyl acetate ratio exceeded 1:4, but the mechanism was not understood determined in this work. Similar changes in lipid production results were found in Wu et al.'s investigations, which examined the lipid yield from *Chlorella* sp. using a mixture of methanol and ethyl acetate as a solvent [47].

3.7.4. Effect of Surfactant Concentration on Lipid Extraction

The effect of surfactant concentration on the lipid extraction process was investigated in the concentration range from 0.1% to 1.4%. Figure 12d depicts the relationship between surfactant concentration and the effectiveness of lipid extraction. It is clearly shown that the lipid yield increases as the HTAC concentration increases until 8%, at which point it slightly decreases.

The surfactant treatment led to a clear difference ranging from 0.1% to 0.5%. When 0.1% of the surfactant was added, the yield of lipid extraction was 6.15%. Then, when the concentration was raised to 0.5%, the lipid extraction was found to be 16.97%. The recovery yield of lipids decreased slightly, with a slight reduction in the trend for concentrations ranging from 1% to 1.4%. The reason for this outcome can be determined by considering the modest range of surfactant concentrations, given that the surfactant resides primarily in the molecular form. The adsorption of the solution at the surface can reach saturation with an increase in the surfactant concentration. On this basis, we selected 0.5% as a reference for surfactant concentration in our experiment, which allowed us to extract 16.97% of the lipid yield.

3.8. Fatty Acid Methyl Ester Profiles of Lipids

The lipids were extracted under the optimal conditions previously described to attain the maximum lipid yield. The FAMEs of the lipids from the pretreated microalgae were obtained via the transesterification process. GC-MS analysis was used to determine the FAME composition of the algal biomass pretreatment, and the results are shown in Figure 13. In this study, FAMEs ranging from C16 to C18 were the most dominant in the FAME mixture made from pretreated microalgae biomass.

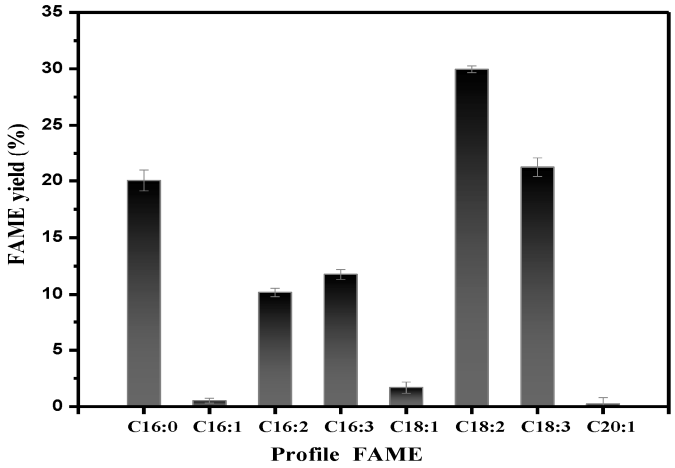

Figure 13. Fatty acid methyl ester profiles from pretreated microalgal biomass.

In summary, *C. pyrenoidosa*'s lipid profile contains eight different fatty acids. The main fatty acids found were Palmitic acid (C16:0); hexadecatrienoic acid (C16:2); 10, 13 504 hexadecatrienoic acid (C16:3); 9,12-octadecadienoic acid (C18:2); and 9,12,15-octadecatrienoic acid (C18:3), which accounted for more than 93.14% of the total fatty acids. Additionally, the fatty acids C16:0, C18:1, C18:2, and C18:3 have been reported to be common fatty acids in plant-based biodiesel, such as that made from spent coffee grounds, canola, soybean, and palm. The methyl ester in the C18 group indicates its ability to be used as fuel, and the amounts of palmitic and stearic acids represent better fuel and ignition properties, respectively [48].

Biodiesel standards (Europe—EN 14214; USA—ASTM 6751) are published to maintain the quality of biodiesel [49,50]. These characteristics include the iodine value (IV), oxidative stability (OS), saponification value (SV), higher heating value (HHV), and value of CN

(which indicates the fuel's ability to be ignited) [51]. We compared the biodiesel produced in the current study to the industrial standards (ASTM D6751 and EN14214) (Table 3).

Table 3. Comparison of biodiesel produced from microalgae using DES supplemented with surfactant and the ASTM specifications of diesel and biodiesel.

Fuel Property	International Standards		Obtained Biodiesel
	EN14214	ASTMD6751	
Degree of unsaturation (DU) (mg $KOHg^{-1}$)	-	-	104.73
Saponification value (SV) (gI $2100g^{-1}$ fat)	-	-	151.09
Iodine value (IV)	≤120	-	114.50
Cetane number (CN)	51–120	>47	56.65
Long-chain saturated factor (LCSF)	-	-	2.00
Kinematic viscosity 40 °C (mm^2 s^{-1})	3.5 to 5.0	1.9 to 6	2.40
Cold filter plugging point (CFPP) (°C)	−20 to 5	-	−10.18
Cloud point (°C)	>4	−3 to −15	5.54
Oxidative stability (OS) (h)	>6	-	4.89
Density ($kg{\cdot}m^{-3}$)	-	0.8 to 0.86	0.65
Higher heating value HHV (MJ Kg^{-1})	-	-	28.90
Fatty acid methyl ester content (wt %)	≥96.50	-	95.59

Both ASTM D6751 and EN 14214 have recommended CN values of >47 and 51–120, respectively. In this investigation, the highest CN value was found to be 56.65, which is in accordance with the industrial standards. The SV, IV, and OS were found to be 151.09 gI $2100g^{-1}$ fat, 114.50, and 4.89 h. The critical parameters for evaluating biodiesel attributes in cold countries are the freezing point (CP) and the cold filter plugging point (CFPP) [52]. In this study, the CFPP and CP values were found to be −10.18 and 5.54, respectively, which are in line with the international standards. The EN 14214 standard for a suitable FAME content is 96.5%; however, ASTM D6751 does not specify FAME content [53]. The FAME content found in this study was 95.59%. The density was found to be 0.65 $kg{\cdot}m^{-3}$, which is not in agreement with the international standard EN14214; however, ASTM standards include no specifications for density. For the biodiesel that meets all other specifications, it has been stated that no determination of density is required, as it will have a density in the desired range [54]. These results support the idea that the lipids extracted by the microalga *C. pyrenoidosa* might be a promising candidate for biodiesel production. However, further experimental studies on the properties of biodiesel made from the microalga *C. pyrenoidosa* are needed.

4. Conclusions

This work aimed to study the ability of DES based on choline chloride and carboxylic acids (FA, AA, and MA) supplemented with surfactants to increase cell wall disruption prior to lipid extraction from microalgae. It was found that the lipid extraction yields from the microalgae were improved via pretreatment. Cell membranes were disrupted using a DES (choline chloride/malonic acid), for which the surfactant aided the lipid recovery process. Additionally, the mechanism of microalgae cell wall disruption via the DES determined using DFT simulation showed several non-covalent interactions between the DES and cellulose. The latter weakens the membrane of the microalgae and thus facilitates the extraction of lipids. Lipid extraction was optimized using a single-factor experiment that included various parameters: time, temperature, the n-butanol/ethyl acetate ratio, and the concentration of surfactant. The best lipid yield (16.97%) was obtained from microalgae biomass pretreatment following an extraction that lasted 60 min at 80 °C with a 1:2 n-butanol/ethyl acetate ratio and the application of 0.5% HTAC. These results support the idea that the lipids obtained from the microalga *C. pyrenoidosa* could be exploited

for biodiesel production. To support this theory, further experimental research on the properties of biodiesel generated from the microalga *C. pyrenoidosa* is needed.

Author Contributions: M.C.M.K.: Conceptualization, Research, Methodology, Validation, Formal Analysis, Data Curation, Writing—Original Draft, Writing—Review and Editing. A.D.T.F.: Data analysis, Review and Editing. N.L.: Visualization, Investigation, Evaluation and Validation. Acquisition of funding and supervision. All authors have read and agreed to the published version of the manuscript.

Funding: This study was financially supported by the Key Laboratory of Well stability and Fluid and Rock mechanism in Oil and Gas reservoir Shaanxi Province, Xi'an Shiyou University (No. WSFRM20210402001), and the Opening Project of the Oil and Gas Field Applied Chemistry of the Key Laboratory of Sichuan Province (No. YQKF202010). Research was conducted in the Laboratory of Enhanced Oil Recovery.

Data Availability Statement: Data used in this manuscript are available upon request.

Conflicts of Interest: The authors declare no conflict of interest.

References

1. Patel, A.; Gami, B.; Patel, P.; Patel, B. Biodiesel production from microalgae *Dunaliella tertiolecta*: A study on economic feasibility on large-scale cultivation systems. *Biomass Convers. Biorefin.* **2023**, *13*, 1071–1085. [CrossRef]
2. Chen, B.; Wan, C.; Mehmood, M.A.; Chang, J.-S.; Bai, F.; Zhao, X. Manipulating environmental stresses and stress tolerance of microalgae for enhanced production of lipids and value-added products—A review. *Bioresour. Technol.* **2017**, *244*, 1198–1206. [CrossRef] [PubMed]
3. Hannon, M.; Gimpel, J.; Tran, M.; Rasala, B.; Mayfield, S. Biofuels from algae: Challenges and potential. *Biofuels* **2010**, *1*, 763–784. [CrossRef] [PubMed]
4. Nagappan, S.; Devendran, S.; Tsai, P.-C.; Dinakaran, S.; Dahms, H.-U.; Ponnusamy, V.K. Passive cell disruption lipid extraction methods of microalgae for biofuel production—A review. *Fuel* **2019**, *252*, 699–709. [CrossRef]
5. Chen, M.; Liu, T.; Chen, X.; Chen, L.; Zhang, W.; Wang, J.; Gao, L.; Chen, Y.; Peng, X. Subcritical co-solvents extraction of lipid from wet microalgae pastes of *Nannochloropsis* sp. *Eur. J. Lipid Sci. Technol.* **2012**, *114*, 205–212. [CrossRef] [PubMed]
6. Ulloa, G.; Coutens, C.; Sánchez, M.; Sineiro, J.; Fábregas, J.; Deive, F.J.; Rodríguez, A.; Núñez, M.J. On the double role of surfactants as microalga cell lysis agents and antioxidants extractants. *Green Chem.* **2012**, *14*, 1044–1051. [CrossRef]
7. Wu, C.; Xiao, Y.; Lin, W.; Zhu, J.; Siegler, H.D.L.H.; Zong, M.; Rong, J. Surfactants assist in lipid extraction from wet *Nannochloropsis* sp. *Bioresour. Technol.* **2017**, *243*, 793–799. [CrossRef]
8. Ozturk, B.; Parkinson, C.; Gonzalez-Miquel, M. Extraction of polyphenolic antioxidants from orange peel waste using deep eutectic solvents. *Sep. Purif. Technol.* **2018**, *206*, 1–13. [CrossRef]
9. Gao, M.-Z.; Cui, Q.; Wang, L.-T.; Meng, Y.; Yu, L.; Li, Y.-Y.; Fu, Y.-J. A green and integrated strategy for enhanced phenolic compounds extraction from mulberry (*Morus alba* L.) leaves by deep eutectic solvent. *Microchem. J.* **2020**, *154*, 104598.
10. Ngatcha, A.D.P.; Muhammad, G.; Lv, Y.; Xiong, W.; Zhao, A.; Xu, J.; Alam, M. Microalgae biomass pre-treatment with deep eutectic solvent to optimize lipid isolation in biodiesel production. *Biomass Convers. Biorefin.* **2022**, *12* (Suppl. S1), 133–143. [CrossRef]
11. Lu, W.; Alam, M.A.; Pan, Y.; Wu, J.; Wang, Z.; Yuan, Z. A new approach of microalgal biomass pretreatment using deep eutectic solvents for enhanced lipid recovery for biodiesel production. *Bioresour. Technol.* **2016**, *218*, 123–128. [CrossRef] [PubMed]
12. Mohan, M.; Naik, P.K.; Banerjee, T.; Goud, V.V.; Paul, S. Solubility of glucose in tetrabutylammonium bromide based deep eutectic solvents: Experimental and molecular dynamic simulations. *Fluid Phase Equilibria* **2017**, *448*, 168–177. [CrossRef]
13. Tommasi, E.; Cravotto, G.; Galletti, P.; Grillo, G.; Mazzotti, M.; Sacchetti, G.; Samorì, C.; Tabasso, S.; Tacchini, M.; Tagliavini, E. Enhanced and Selective Lipid Extraction from the Microalga *P. tricornutum* by Dimethyl Carbonate and Supercritical CO_2 Using Deep Eutectic Solvents and Microwaves as Pretreatment. *ACS Sustain. Chem. Eng.* **2017**, *5*, 8316–8322. [CrossRef]
14. Liang, Y.; Sarkany, N.; Cui, Y. Biomass and lipid productivities of *Chlorella vulgaris* under autotrophic, heterotrophic and mixotrophic growth conditions. *Biotechnol. Lett.* **2009**, *31*, 1043–1049. [CrossRef]
15. Feng, W.; Wang, S.; Duan, X.; Wang, W.; Yang, F.; Xiong, J.; Wang, T.; Wang, C. A novel approach for enhancing lipid recovery for biodiesel production from wet energy biomass using surfactants-assisted extraction. *Renew. Energy* **2021**, *170*, 462–470. [CrossRef]
16. de Almeida Pontes, P.V.; Shiwaku, I.A.; Maximo, G.J.; Caldas Batista, E.A. Choline chloride-based deep eutectic solvents as potential solvent for extraction of phenolic compounds from olive leaves: Extraction optimization and solvent characterization. *Food Chem.* **2021**, *352*, 129346. [CrossRef]
17. Pan, Y.; Alam, M.A.; Wang, Z.; Huang, D.; Hu, K.; Chen, H.; Yuan, Z. One-step production of biodiesel from wet and unbroken microalgae biomass using deep eutectic solvent. *Bioresour. Technol.* **2017**, *238*, 157–163. [CrossRef]
18. Frisch, M.; Trucks, G.; Schlegel, H.B.; Scuseria, G.E.; Robb, M.A.; Cheeseman, J.R.; Scalmani, G.; Barone, V.; Mennucci, B.; Petersson, G.A.; et al. *Gaussian 09 Citation*; Gaussian Inc.: Wallingford, CT, USA, 2013.

19. Binkley, J.S.; Pople, J.A.; Hehre, W.J. Self-consistent molecular orbital methods. 21. Small split-valence basis sets for first-row elements. *J. Am. Chem. Soc.* **1980**, *102*, 939–947.
20. Grimme, S.; Antony, J.; Ehrlich, S.; Krieg, H. A consistent and accurate ab initio parametrization of density functional dispersion correction (DFT-D) for the 94 elements H-Pu. *J. Chem. Phys.* **2010**, *132*, 154104. [CrossRef]
21. Chen, W.; Liu, Y.; Song, L.; Sommerfeld, M.; Hu, Q. Automated accelerated solvent extraction method for total lipid analysis of microalgae. *Algal Res.* **2020**, *51*, 102080. [CrossRef]
22. Howlader, M.S.; Rai, N.; Todd French, W. Improving the lipid recovery from wet oleaginous microorganisms using different pretreatment techniques. *Bioresour. Technol.* **2018**, *267*, 743–755. [CrossRef]
23. Nasirpour, N.; Mousavi, S.M.; Shojaosadati, S.A. A novel surfactant-assisted ionic liquid pretreatment of sugarcane bagasse for enhanced enzymatic hydrolysis. *Bioresour. Technol.* **2014**, *169*, 33–37. [CrossRef] [PubMed]
24. Lu, W.; Alam, A.; Pan, Y.; Nock, W.J.; Wang, Z.; Yuan, Z. Optimization of algal lipid extraction by mixture of ethyl acetate and ethanol via response surface methodology for biodiesel production. *Korean J. Chem. Eng.* **2016**, *33*, 2575–2581. [CrossRef]
25. Loos, E.; Meindl, D. Composition of the cell wall of *Chlorella fusca*. *Planta* **1982**, *156*, 270–273. [CrossRef] [PubMed]
26. Talebi, A.F.; Tabatabaei, M.; Chisti, Y. BiodieselAnalyzer: A user-friendly software for predicting the properties of prospective biodiesel. *Biofuel Res. J.* **2014**, *1*, 55–57. [CrossRef]
27. Suastes-Rivas, J.K.; Hernández-Altamirano, R.; Mena-Cervantes, V.Y.; Gómez, E.J.B.; Chairez, I. Biodiesel production, through intensification and profitable distribution of fatty acid methyl esters by a microalgae-yeast co-culture, isolated from wastewater as a function of the nutrients' composition of the culture media. *Fuel* **2020**, *280*, 118633. [CrossRef]
28. Ijardar, S.P.; Singh, V.; Gardas, R.L. Revisiting the Physicochemical Properties and Applications of Deep Eutectic Solvents. *Molecules* **2022**, *27*, 1368. [CrossRef]
29. Kalhor, P.; Ghandi, K. Deep eutectic solvents for pretreatment, extraction, and catalysis of biomass and food waste. *Molecules* **2019**, *24*, 4012. [CrossRef]
30. Tamafo Fouegue, A.D.; Nono, J.H.; Nkungli, N.K.; Ghogomu, J.N. A theoretical study of the structural and electronic properties of some titanocenes using DFT, TD-DFT, and QTAIM. *Struct. Chem.* **2021**, *32*, 353–366. [CrossRef]
31. Nkungli, N.K.; Ghogomu, J.N. Theoretical analysis of the binding of iron (III) protoporphyrin IX to 4-methoxyacetophenone thiosemicarbazone via DFT-D3, MEP, QTAIM, NCI, ELF, and LOL studies. *J. Mol. Model.* **2017**, *23*, 200. [CrossRef]
32. Mya, K.Y.; Sirivat, A.; Jamieson, A.M. Effect of Ionic Strength on the Structure of Polymer− Surfactant Complexes. *J. Phys. Chem. B* **2003**, *107*, 5460–5466. [CrossRef]
33. Zhou, Y.; Zhang, X.; Yang, X.; Zhang, J. Synergism and Phase Behavior of Alcohol Polyoxyethylene Ether Acetate and Cationic Surfactant-Mixed Systems. *J. Surfactants Deterg.* **2020**, *23*, 145–151. [CrossRef]
34. Belsito, M.; Hill, R.A.; Klaassen, C.D.; Liebler, D.; Marks, J.G., Jr.; Ronald, C. *Decyl Glucoside and Other Alkyl Glucosides as Used in Cosmetics*; Cosmetic Ingredient Review (CIR): Washington, DC, USA, 2011.
35. Fiume, M.M.; Heldreth, B.; Bergfeld, W.F.; Belsito, D.V.; Hill, R.A.; Klaassen, C.D.; Liebler, D.; Marks, J.G.; Shank, R.C.; Slaga, T.J.; et al. Safety assessment of decyl glucoside and other alkyl glucosides as used in cosmetics. *Int. J. Toxicol.* **2013**, *32* (Suppl. S5), 22S–48S. [CrossRef]
36. Lai, Y.S.; De Francesco, F.; Aguinaga, A.; Parameswaran, P.; Rittmann, B.E. Improving lipid recovery from *Scenedesmus* wet biomass by surfactant-assisted disruption. *Green Chem.* **2016**, *18*, 1319–1326. [CrossRef]
37. Callejón, M.J.J.; Medina, A.R.; Sánchez, M.D.M.; Peña, E.H.; Cerdán, L.E.; Moreno, P.A.G.; Grima, E.M. Extraction of saponifiable lipids from wet microalgal biomass for biodiesel production. *Bioresour. Technol.* **2014**, *169*, 198–205. [CrossRef]
38. Do, L.D.; Sabatini, D.A. Aqueous extended-surfactant based method for vegetable oil extraction: Proof of concept. *J. Am. Oil Chem. Soc.* **2010**, *87*, 1211–1220. [CrossRef]
39. Huang, W.-C.; Kim, J.-D. Cationic surfactant-based method for simultaneous harvesting and cell disruption of a microalgal biomass. *Bioresour. Technol.* **2013**, *149*, 579–581. [CrossRef]
40. Arif, M.; Li, Y.; El-Dalatony, M.M.; Zhang, C.; Li, X.; Salama, E.-S. A complete characterization of microalgal biomass through FTIR/TGA/CHNS analysis: An approach for biofuel generation and nutrients removal. *Renew. Energy* **2021**, *163*, 1973–1982. [CrossRef]
41. Pouliot, R.; Germain, L.; Auger, A.; Tremblay, N.; Juhasz, J. Physical characterization of the stratum corneum of an in vitro human skin equivalent produced by tissue engineering and its comparison with normal human skin by ATR-FTIR spectroscopy and thermal analysis (DSC). *Biochim. Biophys. Acta (BBA)-Mol. Cell Biol. Lipids* **1999**, *1439*, 341–352. [CrossRef]
42. Machado, L.; Carvalho, G.; Pereira, R.N. Effects of innovative processing methods on microalgae cell wall: Prospects towards digestibility of protein-rich biomass. *Biomass* **2022**, *2*, 80–102. [CrossRef]
43. Popelier, P.L.A. The QTAIM perspective of chemical bonding. In *The Chemical Bond: Fundamental Aspects of Chemical Bonding*; Wiley-VCH: Weinheim, Germany, 2014; pp. 271–308.
44. Boto, R.A.; Piquemal, J.-P.; Contreras-García, J. Revealing strong interactions with the reduced density gradient: A benchmark for covalent, ionic and charge-shift bonds. *Theor. Chem. Acc.* **2017**, *136*, 139. [CrossRef]
45. Shi, J.; Yu, J.; Pohorly, J.; Young, J.C.; Bryan, M.; Wu, Y. Optimization of the extraction of polyphenols from grape seed meal by aqueous ethanol solution. *J. Food Agric. Environ.* **2003**, *1*, 42–47.
46. Ryckebosch, E.; Muylaert, K.; Foubert, I. Optimization of an analytical procedure for extraction of lipids from microalgae. *J. Am. Oil Chem. Soc.* **2012**, *89*, 189–198. [CrossRef]

47. Wu, J.; Alam, A.; Pan, Y.; Huang, D.; Wang, Z.; Wang, T. Enhanced extraction of lipids from microalgae with eco-friendly mixture of methanol and ethyl acetate for biodiesel production. *J. Taiwan Inst. Chem. Eng.* **2017**, *71*, 323–329. [CrossRef]
48. Knothe, G. "Designer" biodiesel: Optimizing fatty ester composition to improve fuel properties. *Energy Fuels* **2008**, *22*, 1358–1364. [CrossRef]
49. Abomohra, A.E.-F.; Zheng, X.; Wang, Q.; Huang, J.; Ebaid, R. Enhancement of biodiesel yield and characteristics through in-situ solvo-thermal co-transesterification of wet microalgae with spent coffee grounds. *Bioresour. Technol.* **2021**, *323*, 124640. [CrossRef]
50. Anahas, A.M.P.; Muralitharan, G. Characterization of heterocystous cyanobacterial strains for biodiesel production based on fatty acid content analysis and hydrocarbon production. *Energy Convers. Manag.* **2018**, *157*, 423–437. [CrossRef]
51. Shahid, A.; Usman, M.; Atta, Z.; Musharraf, S.G.; Malik, S.; Elkamel, A.; Shahid, M.; Alkhattabi, N.A.; Gull, M.; Mehmood, M.A. Impact of wastewater cultivation on pollutant removal, biomass production, metabolite biosynthesis, and carbon dioxide fixation of newly isolated cyanobacteria in a multiproduct biorefinery paradigm. *Bioresour. Technol.* **2021**, *333*, 125194. [CrossRef]
52. Pedro, G.A.; Amaral, M.S.; Pereira, F.M.; Flumignan, D.L.; Da Rós, P.C.M.; Reis, C.E.R.; Silva, M.B. Highly wet *Chlorella minutissima* biomass for in situ biodiesel production and residual biomass rich in labile carbohydrates. *Bioenergy Res.* **2022**, *15*, 154–165. [CrossRef]
53. Munari, F.; Cavagnino, D. *Determination of Total FAME and Linolenic Acid Methyl Ester in Pure Biodiesel (B100) by GC in Compliance with EN 14103*; Thermo Fisher Scientific: Milan, Italy, 2007.
54. Kumbhar, V.; Pandey, A.; Sonawane, C.R.; El-Shafay, A.; Panchal, H.; Chamkha, A.J. Statistical analysis on prediction of biodiesel properties from its fatty acid composition. *Case Stud. Therm. Eng.* **2022**, *30*, 101775. [CrossRef]